VIP Nanotechnology

DOI: 10.1002/anie.201001308

Electrons as "Invisible Ink": Fabrication of Nanostructures by Local Electron Beam Induced Activation of SiO_x**

*Marie-Madeleine Walz, Michael Schirmer, Florian Vollnhals, Thomas Lukasczyk, Hans-Peter Steinrück, and Hubertus Marbach**

The injection or removal of electrons can be used to trigger chemical processes, such as bond formation or dissociation. In this regard, electrons are an excellent and "clean" tool to modify or engineer the properties of different materials.[1] The availability of localized electron probes, for example, in scanning electron microscopy (SEM), has made it possible to apply electron-induced processes on the nanometer and subnanometer scale.[2–6] This approach can be used to target the generation of extremely small, pure nanostructures with lithographic control, which is one of the main goals in nanotechnology.

The starting point of our study was the electron beam induced deposition (EBID) technique. The principle of EBID is outlined in Scheme 1 a–c. A highly focused electron beam locally decomposes adsorbed precursor molecules to leave a deposit of nonvolatile fragments. The importance of EBID recently increased since it superseded focused ion beam processing as a method to repair lithographic masks in the semiconductor industry.[7] The underlying physical and chemical principles of electron-induced bond making and breaking are in general also of great interest for important technological applications such as electron beam lithography (EBL), which is the standard method of generating the masks for UV lithography.

As there is a large variety of precursor molecules and there are nearly no restrictions in regard to the substrate, EBID allows almost every combination of deposit material and substrate to be targeted.[4–6] As a prototype example for conductive structures on an insulating material, our aim here was to generate clean iron nanostructures on a SiO_x layer on Si(001). Scheme 1 a–c depicts a schematic representation of the EBID process in which iron pentacarbonyl ($[Fe(CO)_5]$) is locally decomposed by electrons to generate a pure iron deposit.

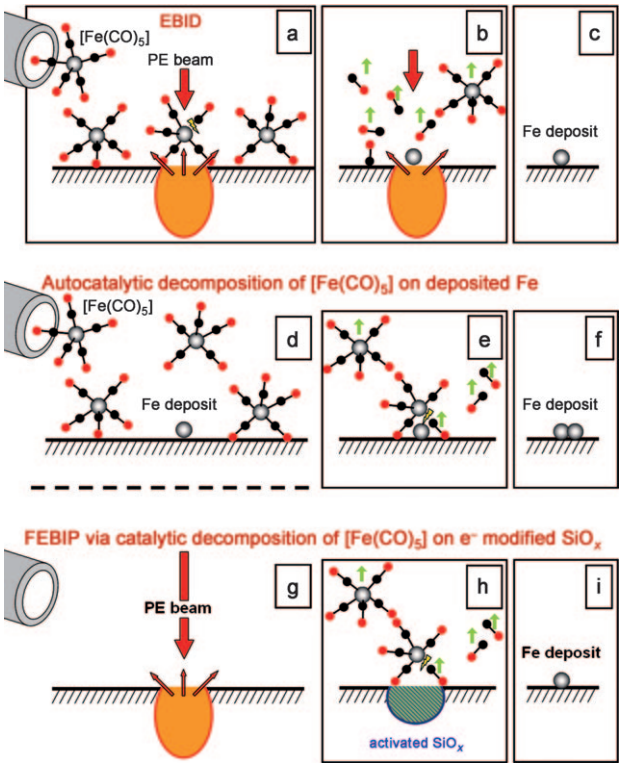

Scheme 1. Three different decomposition routes of $[Fe(CO)_5]$. a–c) Ideal EBID process: a) Dosage and adsorption of $[Fe(CO)_5]$; local exposure of adsorbed molecules to the primary electron (PE) beam and emitted back-scattered and secondary electrons (created within the orange cone). b) Electron-induced decomposition of $[Fe(CO)_5]$ into volatile fragments (e.g., CO) and nonvolatile fragments (e.g., Fe) and desorption of unexposed, intact molecules. c) Resulting Fe deposit. d–f) Autocatalytic decomposition on already deposited Fe: d) $[Fe(CO)_5]$ dosage onto a surface already covered with predeposited Fe. e) Autocatalytic decomposition of $[Fe(CO)_5]$ on predeposited Fe. f) Enlarged Fe deposit. g–i) Decomposition of $[Fe(CO)_5]$ on electron-modified, activated SiO_x (300 nm) on Si(001). g) Irradiation of the SiO_x layer with the primary electron beam. h) Decomposition of $[Fe(CO)_5]$ on the activated SiO_x sample. i) Fe deposit.

The routine focusing of electron beams down to the nanometer regime means that EBID is capable of producing arbitrarily shaped nanostructures, which can be as small as 1–3 nm for ultrathin samples.[3]

Organometallic precursors have mostly been used for the generation of metallic nanostructures by EBID. Up to now,

[*] M.-M. Walz, M. Schirmer, F. Vollnhals, T. Lukasczyk, Prof. Dr. H.-P. Steinrück, Dr. H. Marbach
Lehrstuhl für Physikalische Chemie II
Universität Erlangen-Nürnberg
Egerlandstrasse 3, 91058 Erlangen (Germany)
Fax: (+49) 9131-852-8867
E-mail: marbach@chemie.uni-erlangen.de
and
Interdisciplinary Center for Molecular Materials
Universität Erlangen-Nürnberg
Egerlandstrasse 3, 91058 Erlangen (Germany)

[**] This work was supported by the DFG (grant MA 4246/1-1), COST Action CM0601, COST Action D41, and by the Cluster of Excellence "Engineering of Advanced Materials". We thank Stefan Tampier and Dr. Matthias Moll from the Institute of Inorganic Chemistry (University Erlangen-Nürnberg) for technical assistance.

Supporting information for this article is available on the WWW under http://dx.doi.org/10.1002/anie.201001308.

© 2010 Wiley-VCH Verlag GmbH & Co. KGaA, Weinheim

the vast majority of EBID experiments were performed in a high vacuum (HV) environment, which results in a typical metal content of only 15 to 60 % in the corresponding deposits (for example, see Refs. [8,9]), with carbon and oxygen being the main contaminations. The carbon content is attributed to the decomposition of carbon-containing fragments from the precursor gas or of hydrocarbons in the residual gas in the HV chamber. This effect can also be exploited directly to generate carbonaceous deposits, for example, as templates for the growth of polymer brushes.[10] To avoid such contaminations, we apply a "surface-science" approach, namely EBID under ultrahigh vacuum (UHV) conditions on well-defined samples.[11–13] By following this approach and using $[Fe(CO)_5]$ we were able to produce very clean iron nanostructures with a metal content of greater than 95 % and partially with dimensions below 10 nm.[11,12] It was found in these studies that the surface of the sample played an active part in the deposition process. Furthermore, the long-range order and purity of the substrate can also strongly influence the composition and morphology of the deposits produced by EBID.[11,12]

Herein we report the local activation of an oxide surface by a focused electron beam, such that $[Fe(CO)_5]$ is catalytically decomposed at irradiated regions of the surface at room temperature. First we discuss results obtained using the "classical" EBID protocol, that is, by exposing the surface to the electron beam while dosing $[Fe(CO)_5]$. We then demonstrate that Fe deposits can also be produced by first activating certain surface regions with the electron beam and then exposing the surface to the precursor gas in a second step. The sample is an industrial standard 300 nm SiO_x layer on a Si(001) substrate.

Figure 1 a shows a representative section of a line with a total length of 45 μm written by EBID; the electron line dose was 1.9 $\mu C cm^{-1}$ and the nominal $[Fe(CO)_5]$ background pressure was 3×10^{-7} mbar (the actual pressure was higher since the dosing nozzle was pointing directly at the surface). The resulting line, with a diameter of roughly 45 nm, appears darker than the rest of the surface in the SEM image. As a next processing step, the surface was further exposed to the precursor gas without additional irradiation by the electron beam. The corresponding SEM images are depicted in Figure 1 b–g for representative parts of the line equivalent to that in Figure 1 a. A continuous transition from the dark line at 0 minutes to increasingly brighter and broader lines occurs as the $[Fe(CO)_5]$ dosage increases after the EBID process, with the substructure of the lines changing from a granular morphology at 30 minutes to larger, cubelike structures at 180 minutes.

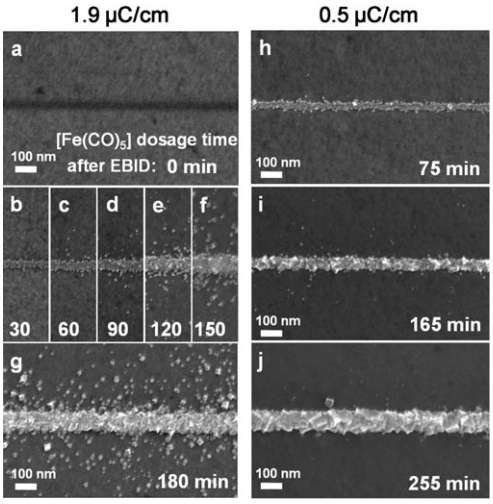

Figure 1. Fe line deposits on SiO_x (300 nm) on Si(001), generated by utilizing two different electron line doses and different additional $[Fe(CO)_5]$ dosage times after the conventional EBID process, as denoted in the corresponding images. a–g) Line dose 1.9 $\mu C cm^{-1}$; h–j) line dose 0.5 $\mu C cm^{-1}$ (see the Supporting Information for an animated sequence and the main text for further details).

The width of the line after 180 minutes (Figure 1 g) is less than 95 nm. In addition to the lines, scattered structures develop in the immediate environment, that is, in areas not directly irradiated by the primary electron beam. These structures also grow in number and size as the gas exposure time increases.

These scattered structures are caused by the back-scattered electron (BSE) proximity effect.[6] The observed growth of the line structure upon postexposure to the precursor gas is attributed to local autocatalytic decomposition of $[Fe(CO)_5]$ at the EBID structures. The basic principle of the autocatalytic growth is that small amounts of iron deposited by EBID act as seeds for further growth (Scheme 1 d–f).

In addition to the postexposure time to the precursor gas, the amount of iron predeposited by EBID is expected to act as a parameter for controlling the size and morphology of the autocatallytically grown iron structures. To verify this hypothesis, we compare the structures obtained for a line dose of 1.9 $\mu C cm^{-1}$ and 0.5 $\mu C cm^{-1}$ under otherwise identical experimental conditions. The corresponding line sections are shown in Figure 1 h–j. While the main observations, namely, the changes in growth and morphology with increasing gas dose, are reproduced, the scattered features are strongly reduced. This behavior demonstrates that the total electron dose during EBID, and consequently the amount and distribution of predeposited iron, indeed strongly influences the shape and size of the autocatalytically grown structures. Longer gas exposure times lead to deposits with a cubic shape, which is consistent with the growth of pure bcc α-iron crystals.[14,15] Indeed, local Auger electron spectroscopy indicates an iron content of greater than 95 % (see the Supporting Information).

Iron deposits on SiO_x are expected to appear brighter than the substrate in SEM because of their higher atomic number/mass.[16] Thus, the nature of the dark line in Figure 1 a has to be further discussed: The fact that a darkening of the SiO_x surface is also observed during acquisition of a normal scanning electron micrograph indicates that the appearance of the dark line in Figure 1 a could at least partially be due to irradiation by the electron beam. The amount of iron deposited during EBID at the position of the line is clearly so low that it does not contribute significantly to the observed contrast.

 © 2010 Wiley-VCH Verlag GmbH & Co. KGaA, Weinheim

These results demonstrate unequivocally that it is possible to grow clean iron nanostructures autocatalytically with controlled shape and morphology (granular or crystalline) on SiO_x at room temperature. The seeds for the growth process consist of very small amounts of iron deposited by EBID prior to the additional exposure to the precursor gas. The application of higher partial pressures of $[Fe(CO)_5]$ after the EBID process is expected to speed up the overall growth process. The autocatalytic growth can, however, also present a major complication: particularly for longer writing processes by EBID, the structures generated at the beginning of the EBID experiment are exposed to the precursor gas for a longer time than structures generated at the end and are, therefore, subject to enhanced autocatalytic deposition.

As discussed above, the amount of deposited iron required as a seed for the autocatalytic growth process is apparently very small. Also, a darkening of the surface, as seen in Figure 1 a, is generally observed upon exposure to the electron beam. Thus, one might suspect that the substrate itself is also locally modified by the electron beam in such a way that the decomposition of $[Fe(CO)_5]$ is promoted. The basic idea of such a process is outlined in Scheme 1 g–i. To test this concept the surface was first irradiated by the electron beam under UHV conditions (background pressure $\leq 1.5 \times 10^{-10}$ mbar), namely, without the simultaneous dosage of the iron precursor. Then, $[Fe(CO)_5]$ was dosed for a certain period of time (here 270 minutes) at a background pressure of 3×10^{-7} mbar. Figure 2 shows the corresponding SEM images for increasing electron line doses, and demonstrates the growth of line structures in the irradiated regions.

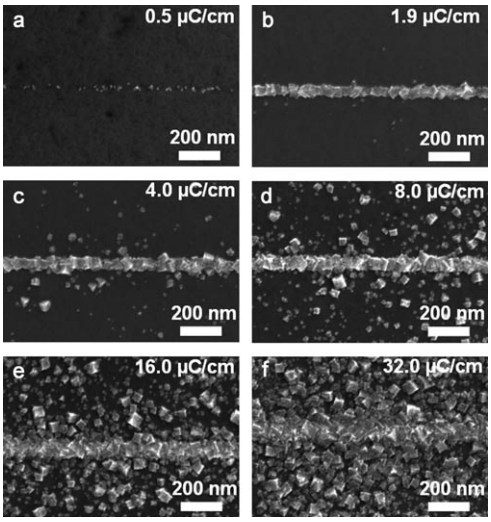

Figure 2. Fe line deposits on SiO_x (300 nm) on Si(001) generated by the activation of the SiO_x with different electron line doses and a subsequent $[Fe(CO)_5]$ dosage for 270 minutes in each case. The applied electron line doses are noted in the corresponding images.

In analogy to chemical photography or classical UV lithography this process can be divided in two steps:[17] 1) "exposure" in the form of a local alteration/activation of the surface by electron irradiation, 2) "development" by dosage of the precursor, which is then decomposed solely at surface regions irradiated by the electron beam (see Scheme 1 g–i). The resulting Fe deposits then serve as seeds for the autocatalytic decomposition of $[Fe(CO)_5]$ at room temperature (see Scheme 1 d–f), which lead to a growth of continuous iron structures at the positions predefined by the electron beam. By choosing the correct electron dose and gas exposure, the formation of scattered structures by the BSE proximity effect can be nearly completely suppressed by using our approach and well defined lines are formed (for example, Figure 2 b, width below 50 nm). Furthermore, the problem of uncontrolled autocatalytic growth, which occurs if the Fe seeds are produced by EBID, is overcome here, since exposure to the precursor occurs solely after irradiation with electrons.

The "activated" sites are attributed to oxygen vacancies generated by electron-induced desorption of oxygen by a Knotek–Feibelman mechanism,[18,19] as has been suggested by Pfnür et al. for ultrathin SiO_x films.[20] In their studies, the generation of nanostructures was achieved by electron beam assisted selective thermal desorption (EBSTD) lithography, a method introduced by Watanabe and co-workers.[21] The first processing step in EBSTD, namely, the irradiation of an ultrathin SiO_x film on a Si substrate with a focused electron beam, is interpreted as a local reduction of SiO_2 to SiO.

The subsequent development step is then performed by thermal desorption of the SiO species, that is, by heating the sample, thereby resulting in surface regions free of oxide, namely, regions with exposed bare Si substrate. This method is apparently restricted to ultrathin silicon oxide films. On the basis of these findings we propose that SiO is the active species for the initial decomposition of $[Fe(CO)_5]$, which is then succeeded by autocatalytic decomposition once the first Fe seeds are formed. Autocatalytic thermal decomposition of $[Fe(CO)_5]$ on silicon samples at specifically modified sites (for example, by Ga^+ impact) has occasionally been reported in the past.[22] However, one of the major drawbacks was the requirement of elevated temperatures to generate a deposit, while the deposits reported here are grown at room temperature.

It is important to note that we reproduced the main findings several times on different samples, in particular also on samples "freshly" introduced into the UHV chamber without any previous exposure to $[Fe(CO)_5]$. Thus, we can rule out that the electron-induced decomposition of adsorbed precursor molecules remaining from a previous experiment is the main cause of the observed effect. The autocatalytic growth of iron upon prolonged exposure to $[Fe(CO)_5]$ at room temperature appears to occur solely under UHV conditions.[12,14] In contrast, increased sample temperatures, mostly around 450 K, are reported for HV conditions.[23]

Furthermore, the electron-induced activation was either strongly reduced or completely suppressed for samples with high levels of carbon contamination; a sufficiently clean surface is required, again indicating the importance of maintaining a clean surface under UHV conditions. In regard to a possible deactivation of the electron-beam irradiated areas by decomposition of residual gases, we

 © 2010 Wiley-VCH Verlag GmbH & Co. KGaA, Weinheim

found that the irradiated areas were still active in UHV for at least two days.

The described new procedure for the generation of clean Fe nanostructures belongs to the methods denoted as focused electron beam induced processing (FEBIP), which also include the EBID technique; it certainly has the potential for interesting applications. Other molecules might also dissociate at the areas activated by electron-beam irradiation, with especially promising candidates being the metal carbonyl compounds $[Cr(CO)_6]$,[23] $[Ni(CO)_4]$, and $[Co_2(CO)_8]$.[5] A next step might be to use other oxide substrates, such as TiO_2, for the local activation. Another important factor is the optimization of the process parameters, for example, in respect to the achievable size of the nanostructures. Thus, we propose that our novel FEBIP maskless lithographic technique is a promising tool for the engineering of metallic nanostructures on insulating substrates. In comparison to EBID, the new FEBIP process described here has the advantage that no scattering of the electrons occurs in an already formed deposit, that is, no additional unintended deposits in proximity to the irradiated area are generated by the forward scattered electron proximity effect.[6,9,24] Furthermore, it should also work well with mask techniques used in the semiconductor industry. Considering the relatively low electron doses required (and the possibility that UV light might do the job just as well)[25] in combination with higher precursor gas pressures, one might even envisage industrial applications, where the actual size of the deposits can be controlled by the precursor dosage. Provided that it is indeed the proposed Knotek–Feibelman mechanism[18] which mostly accounts for the local activation, the present size limitations in electron-beam lithography that arise from effects triggered by secondary low energy electrons might, at least partly, also be overcome.

In conclusion, we have presented a novel two-step process to locally generate iron nanostructures on a commercial 300 nm SiO_x on Si(001) sample at room temperature. In the first step, the surface is locally activated by a 3 nm wide electron beam. The second step comprises the development of the activated structures by dosing an organometallic precursor (namely $[Fe(CO)_5]$), which then decomposes and grows autocatalytically to form pure Fe nanocrystals until the precursor supply is stopped. In a more vivid picture, one might think of the whole process as writing with invisible ink in the irradiation step, which is then made visible by the development step. Besides the fantasy-stimulating application to write secret nanomessages in UHV, the described effect might be the starting point for a whole new way to generate nanostructures.

Experimental Section

All experiments were performed in a UHV chamber system (Multiscanlab Omicron Nanotechnology, Germany) with a base pressure of less than 2×10^{-10} mbar. The main component of the analysis chamber is a UHV-compatible electron column (Leo Gemini), which enables SEM with a resolution better than 3 nm. The precursor, iron pentacarbonyl $[Fe(CO)_5]$, was purchased from Acros Organics (Belgium) and ABCR GmbH & Co. KG (Germany), with a specified purity of 99.5%. The 300 nm SiO_x on Si(001) substrate (thermal oxide; length: 10 mm; width: 2 mm; thickness: 0.38 mm; *p*-type, $\rho =$ 1–20 Ωcm, delivered with Illmar P4 protective coating) was purchased from CrysTec GmbH (Germany). The substrate was sonicated sequentially under atmospheric conditions in acetone, isopropanol, and distilled water for at least 5 minutes, to remove the carbon-containing protective coating. The substrate was not further cleaned or annealed after it was introduced into the UHV. All EBID and FEBIP experiments were carried out with a primary electron beam energy of 15 kV and a beam current of 400 pA.

Received: March 4, 2010

Keywords: crystal growth · electron microscopy · iron · nanotechnology · silicon oxide

[1] a) A. A. C. Papageorgiou, C. L. Pang, Q. Chen, G. Thornton, *ACS Nano* **2007**, *1*, 409; b) A. Gölzhäuser, W. Eck, W. Geyer, V. Stadler, T. Weimann, P. Hinze, M. Grunze, *Adv. Mater.* **2001**, *13*, 803; c) W. Eck, A. Kuller, M. Grunze, B. Volkel, A. Gölzhäuser, *Adv. Mater.* **2005**, *17*, 2583; d) A. Turchanin, A. Beyer, C. T. Nottbohm, X. H. Zhang, R. Stosch, A. Sologubenko, J. Mayer, P. Hinze, T. Weimann, A. Gölzhäuser, *Adv. Mater.* **2009**, *21*, 1233; e) T. Hamann, E. Bohler, P. Swiderek, *Angew. Chem.* **2009**, *121*, 4715; *Angew. Chem. Int. Ed.* **2009**, *48*, 4643; f) R. D. Ramsier, J. T. Yates, *Surf. Sci. Rep.* **1991**, *12*, 246.

[2] a) W. F. van Dorp, C. W. Hagen, P. A. Crozier, P. Kruit, *Nanotechnology* **2008**, *19*, 225305; b) S. Matsui, K. Mori, *J. Vac. Sci. Technol. B* **1986**, *4*, 299; c) A. N. Broers, W. W. Molzen, J. J. Cuomo, N. D. Wittels, *Appl. Phys. Lett.* **1976**, *29*, 596; d) H. W. P. Koops, R. Weiel, D. P. Kern, T. H. Baum, *J. Vac. Sci. Technol. B* **1988**, *6*, 477.

[3] a) W. F. van Dorp, B. van Someren, C. W. Hagen, P. Kruit, *Nano Lett.* **2005**, *5*, 1303; b) L. van Kouwen, A. Botman, C. W. Hagen, *Nano Lett.* **2009**, *9*, 2149.

[4] S. J. Randolph, J. D. Fowlkes, P. D. Rack, *Crit. Rev. Solid State Mater. Sci.* **2006**, *31*, 55.

[5] I. Utke, P. Hoffman, J. Melngailis, *J. Vac. Sci. Technol. B* **2008**, *26*, 1197.

[6] W. F. van Dorp, C. W. Hagen, *J. Appl. Phys.* **2008**, *104*, 081301.

[7] K. Edinger, H. Becht, J. Bihr, V. Boegli, M. Budach, T. Hofmann, H. W. P. Koops, P. Kuschnerus, J. Oster, P. Spies, B. Weyrauch, *J. Vac. Sci. Technol. B* **2004**, *22*, 2902.

[8] a) I. Utke, P. Hoffmann, R. Berger, L. Scandella, *Appl. Phys. Lett.* **2002**, *80*, 4792; b) A. Botman, J. J. L. Mulders, C. W. Hagen, *Nanotechnology* **2009**, *20*, 372001.

[9] Y. M. Lau, P. C. Chee, J. T. L. Thong, V. Ng, *J. Vac. Sci. Technol. A* **2002**, *20*, 1295.

[10] M. Steenackers, R. Jordan, A. Küller, M. Grunze, *Adv. Mater.* **2009**, *21*, 2921.

[11] T. Lukasczyk, M. Schirmer, H.-P. Steinrück, H. Marbach, *Small* **2008**, *4*, 841.

[12] T. Lukasczyk, M. Schirmer, H.-P. Steinrück, H. Marbach, *Langmuir* **2009**, *25*, 11930.

[13] O. Guise, H. Marbach, J. Levy, J. Ahner, J. T. Yates, *Surf. Sci.* **2004**, *571*, 128.

[14] W. Zhang, M. Shimojo, M. Takeguchi, K. Furuya, *J. Mater. Sci.* **2006**, *41*, 2577.

[15] A. F. Holleman, E. Wiberg, N. Wiberg, *Holleman-Wiberg, Lehrbuch der Anorganischen Chemie*, *Vol. 101*, Walter de Gruyter, Berlin, **1995**.

[16] L. Reimer, *Scanning Electron Microscopy*, Springer, Heidelberg, **1998**.

[17] *Springer handbook of nanotechnology*, (Ed. B. Bhushan), Springer, Berlin, **2006**.

[18] M. L. Knotek, P. J. Feibelman, *Phys. Rev. Lett.* **1978**, *40*, 964.

[19] H. Niehus, W. Losch, *Surf. Sci.* **1981**, *111*, 344.

 © 2010 Wiley-VCH Verlag GmbH & Co. KGaA, Weinheim

[20] a) T. Block, H. Pfnür, *J. Appl. Phys.* **2008**, *103*, 064303; b) H. Pfnür, V. Zielasek, C. Tegenkamp, T. Block, Z. Kallassy, *Mater. Sci.-Pol.* **2005**, *23*, 861.
[21] a) S. Fujita, S. Maruno, H. Watanabe, M. Ichikawa, *J. Vac. Sci. Technol. A* **1997**, *15*, 1493; b) H. Watanabe, K. Fujita, M. Ichikawa, *Appl. Phys. Lett.* **1997**, *70*, 1095.
[22] a) D. P. Adams, T. M. Mayer, B. S. Swartzentruber, *Appl. Phys. Lett.* **1996**, *68*, 2210; b) R. L. Kubena, F. P. Stratton, T. M. Mayer, *J. Vac. Sci. Technol. B* **1988**, *6*, 1865.
[23] R. R. Kunz, T. M. Mayer, *J. Vac. Sci. Technol. B* **1988**, *6*, 1557.
[24] Y. F. Guan, J. D. Fowlkes, S. T. Retterer, M. L. Simpson, P. D. Rack, *Nanotechnology* **2008**, *19*, 505302.
[25] C. Fiori, R. A. B. Devine, *Phys. Rev. Lett.* **1984**, *52*, 2081.

 © 2010 Wiley-VCH Verlag GmbH & Co. KGaA, Weinheim